



ELSEVIER

April 1997

Materials Letters 30 (1997) 351–355

**MATERIALS
LETTERS**

Crystallization and magnetic properties of melt-spun two-phase nanocrystalline Nd–Fe–B alloy

Shan-dong Li, Wen-sheng Sun^{*}, Ming-xiu Quan*National Key Lab for RSA, Institute of Metal Research, Academia Sinica, Shenyang 110015, China*

Received 3 July 1996; revised 6 September 1996; accepted 10 September 1996

Abstract

A new type of permanent magnet alloy with composition $\text{Nd}_{9.32}\text{Fe}_{85.32}\text{B}_{5.36}$ has been prepared by a melt spinning method. After optimized annealing of the initial amorphous alloy, high magnetic properties are obtained in the isotropic specimens. Remanence, energy product and intrinsic coercivity are 1.09 T, 153.6 kJ m^{-3} and 400 kA m^{-1} , respectively. The samples consist of two phases, a matrix of nanometer-sized hard magnetic $\text{Nd}_2\text{Fe}_{14}\text{B}$ phase (about 40 nm) together with numerous α -iron particles (about 20 nm) embedded in it. The crystallization behavior for amorphous samples has been studied. The results indicate that the α -iron initially precipitates from the amorphous matrix, and at higher annealing temperatures the crystallization of the $\text{Nd}_2\text{Fe}_{14}\text{B}$ phase occurs. No metastable phase was observed in all heat treatments. Although the volume fraction of the magnetically soft α -iron is about 30 vol%, the second quadrant of the J - H loop is typical of a magnetically soft hard material. The role of exchange coupling between the magnetically soft grain and the magnetically hard grain is discussed.

Keywords: Nd–Fe–B magnets; Nanometer two-phase permanent magnet materials; Exchange coupling; Remanence enhancement; Melt spinning; Rare earth; Permanent magnetic materials

1. Introduction

The discovery of a new permanent magnet alloy, $\text{Nd}_2\text{Fe}_{14}\text{B}$, has resulted in much attention for this material due to its excellent magnetic properties [1–3]. A typical value for the remanence, J_r is 0.8 T. According to the Stoner–Wohlfarth theory [4], the remanence rate $m_r = J_r/J_s$ for randomly oriented single-domain particles with no interaction with one another, is 0.5. However, high remanence behavior

(HIREM) in isotropic specimens was recently [5–7] reported. Their remanence rates were higher than 0.5; some specimens were even in excess of 0.8. Theoretical results [8–10] showed that the HIREM phenomenon arises from an intergranular magnetic exchange interaction in nanostructured specimens. Clemente et al. [11] reported that the enhancement of remanence required a microstructure with a fairly uniform distribution of randomly oriented fine equiaxed grains. In addition, the predominant microstructure should be substantially free from any intergranular phases, either crystalline or amorphous, which would inhibit the exchange interaction between adjacent grains. With decreasing the grain

^{*} Corresponding author.

size, the exchange interaction between neighboring grains increases. When the grain size of a magnetically soft phase is about 2 times the width of a Bloch domain wall of a magnetically hard phase, the irreversible nucleation in the magnetically soft phase is suppressed by exchange interaction. As a result, a significant coercivity can be obtained. In this paper, the $\text{Nd}_2\text{Fe}_{14}\text{B}/\alpha\text{-Fe}$ microstructure system was chosen to study its crystallization behavior and magnetic properties.

2. Experimental methods

An ingot of nominal composition $\text{Nd}_{9.32}\text{-Fe}_{85.32}\text{B}_{5.36}$ was melted 3 times for homogenization in a water-cooled copper boat under argon. The alloy was solidified rapidly by melt-spinning onto a molybdenum roll, at circumferential speeds, V_r , of 36 m/s, in a 10^{-5} Torr vacuum melt-spinning apparatus. Circular ribbon samples were selected and the magnetic properties measured by use of a pulse magnetometer with a maximum field of 6 T. The microstructural evolution was characterized by X-ray diffraction and transmission electron microscopy. Differential thermal analysis was used to analyze the crystallization behavior of the specimens.

3. Results and discussion

3.1. Crystallization behavior of amorphous $\text{Nd}_{9.32}\text{Fe}_{85.32}\text{B}_{5.36}$ ribbon

Under optimized rapid-solidification conditions, amorphous specimens were obtained (Fig. 1 and Fig.

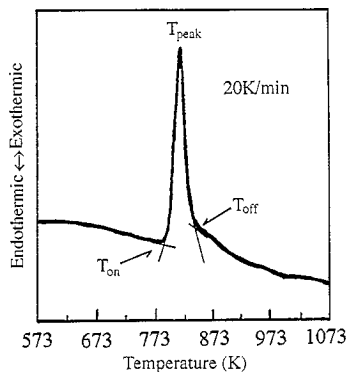


Fig. 1. DTA trace of a melt-spun $\text{Nd}_{9.32}\text{Fe}_{85.32}\text{B}_{5.36}$ ribbon.

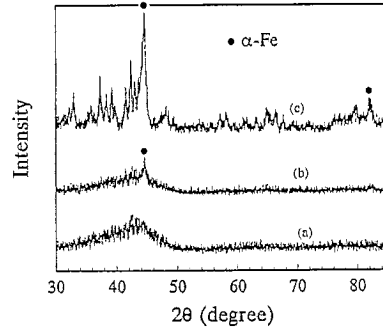


Fig. 2. XRD patterns of a specimen at different annealing temperatures: (a) as-quenched, (b) 813 K, (c) 903 K.

2a). Crystallization behavior was determined by differential thermal analysis (DTA). The DTA trace shown in Fig. 1 indicates that only one exothermic peak exists, which is different from that reported by Withanawansam et al. [12]. They reported that there is a phase transformation during annealing, showing the presence of a metastable phase with composition $\text{Y}_3\text{Fe}_{62}\text{B}_{14}$. This metastable material did not exhibit permanent magnetic properties due to its cubic structure (no uniaxial magnetocrystalline anisotropy). In our work, this metastable phase was not observed. We found that α -iron phase precipitates first from the amorphous matrix at T_{on} (see Fig. 1), where T_{on} stands for the onset temperature of crystallization, then the $\text{Nd}_2\text{Fe}_{14}\text{B}$ phase is formed accompanied by grain growth of α -iron at T_{off} , the completion temperature of crystallization (see Fig. 1 and Fig. 2b, 2c). A two-phase microstructure ($\alpha\text{-Fe} + \text{Nd}_2\text{Fe}_{14}\text{B}$) is present after the complete crystallization.

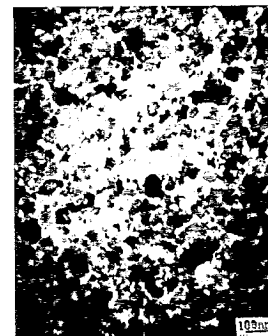


Fig. 3. TEM image of $\text{Nd}_{9.32}\text{Fe}_{85.32}\text{B}_{5.36}$ as quenched ribbon showing the two-phase microstructure. Small grain is $\alpha\text{-Fe}$ and the large one is $\text{Nd}_2\text{Fe}_{14}\text{B}$ phase.

3.2. The microstructure and magnetic properties

The microstructure of the crystallized melt-spun ribbons, as observed by TEM is shown in Fig. 3, and is comprised of two phases. One is the magnetically hard $\text{Nd}_2\text{Fe}_{14}\text{B}$ phase (≈ 40 nm in diameter), the other is a magnetically soft α -iron phase (≈ 20 nm in diameter), and the volume fraction of these two phases, determined by X-ray analysis, is 69 vol% and 31 vol%, respectively. Although a substantial fraction of the α -iron was evident from the microstructure, the hysteresis loop obtained by use of a pulse magnetometer shows typical hard magnetic behavior (see Fig. 4).

The relationship between the magnetic properties and the mean grain sizes (see Table 1) shows that the residual polarization is in excess of 0.9 T; for specimen No. 1 the value even reached 1.09 T, which is higher than the value predicted from the Stoner–Wohlfarth theory [4]. This implies that HIREM behavior occurs in this nanostructured material. According to Skomski's theoretical results [8], the irreversible nucleation is suppressed when the grain size of a magnetically soft phase is about two times that of the Bloch domain wall width of a magnetically hard phase, and gives rise to a remarkable nucleation field. Schrefl et al. [9] reported that for ultra fine particles, the magnetocrystalline anisotropy constant, K_1 , is different from that of a coarse-grained material due to the presence of strong exchange interactions between grains. This inhomogeneous state results in spontaneous polarization deviating from individual easy magnetization axes near the grain boundary in the residual magnetization state. As a result, the polarization fraction parallel to the applied field direction is enhanced. In addition, with decreasing the grain size, the volume fraction of an inhomogeneous magnetization state increases and the residual

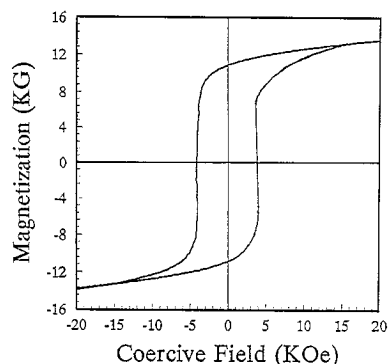


Fig. 4. Typical $J-H$ loop for $\text{Nd}_{9.32}\text{Fe}_{85.32}\text{B}_{5.36}$ annealed at 903 K. $J_r = 1.09$ T and $(BH)_{\max} = 153.6$ kJ m^{-3} .

polarization is enhanced. The high remanence in this alloy can be attributed to the generation of an extremely fine microstructure with both $\text{Nd}_2\text{Fe}_{14}\text{B}$ grains and α -iron particles sufficiently small to be strongly affected by magnetic exchange interactions between neighboring grains. The effects of grain sizes on the remanent magnetization and intrinsic coercivity are shown in Fig. 5a and 5c. The result shown in Fig. 5b indicates that the residual polarization increases monotonously with decreasing grain size of both α -Fe and $\text{Nd}_2\text{Fe}_{14}\text{B}$. Every line in Fig. 5b means a constant remanence resulted from the different grain size of $\text{Nd}_2\text{Fe}_{14}\text{B}$ and α -Fe. However, there exists a ‘‘plateau region’’ for the intrinsic coercivity where high coercivity can be obtained (see Fig. 5c), when the grain size is larger or smaller than this range, the intrinsic coercivity would deteriorate. Therefore, excellent magnetic properties can be obtained as long as the grain sizes of both $\text{Nd}_2\text{Fe}_{14}\text{B}$ and α -iron are controlled in a special range. This range for our specimens is about 15–47 nm.

Some researchers found [6,13] that there is a linear relationship between residual polarization, J_r ,

Table 1
Relationship between the magnetic properties and the mean grain sizes, D , of α -Fe and $\text{Nd}_2\text{Fe}_{14}\text{B}$ phases

No.	$D_{\alpha\text{-Fe}}$ (nm)	D_{ϕ} ^a (nm)	J_r (T)	H_c (A m^{-1})	$(BH)_{\max}$ (kJ m^{-3})
1	15	38	1.090	334.4	153.6
2	18	39	0.903	404.0	83.68
3	20	44	0.943	407.2	97.68
4	20	47	0.975	305.6	114.24
5	25	41	0.962	396.8	101.92

^a ϕ stands for $\text{Nd}_2\text{Fe}_{14}\text{B}$ phase.

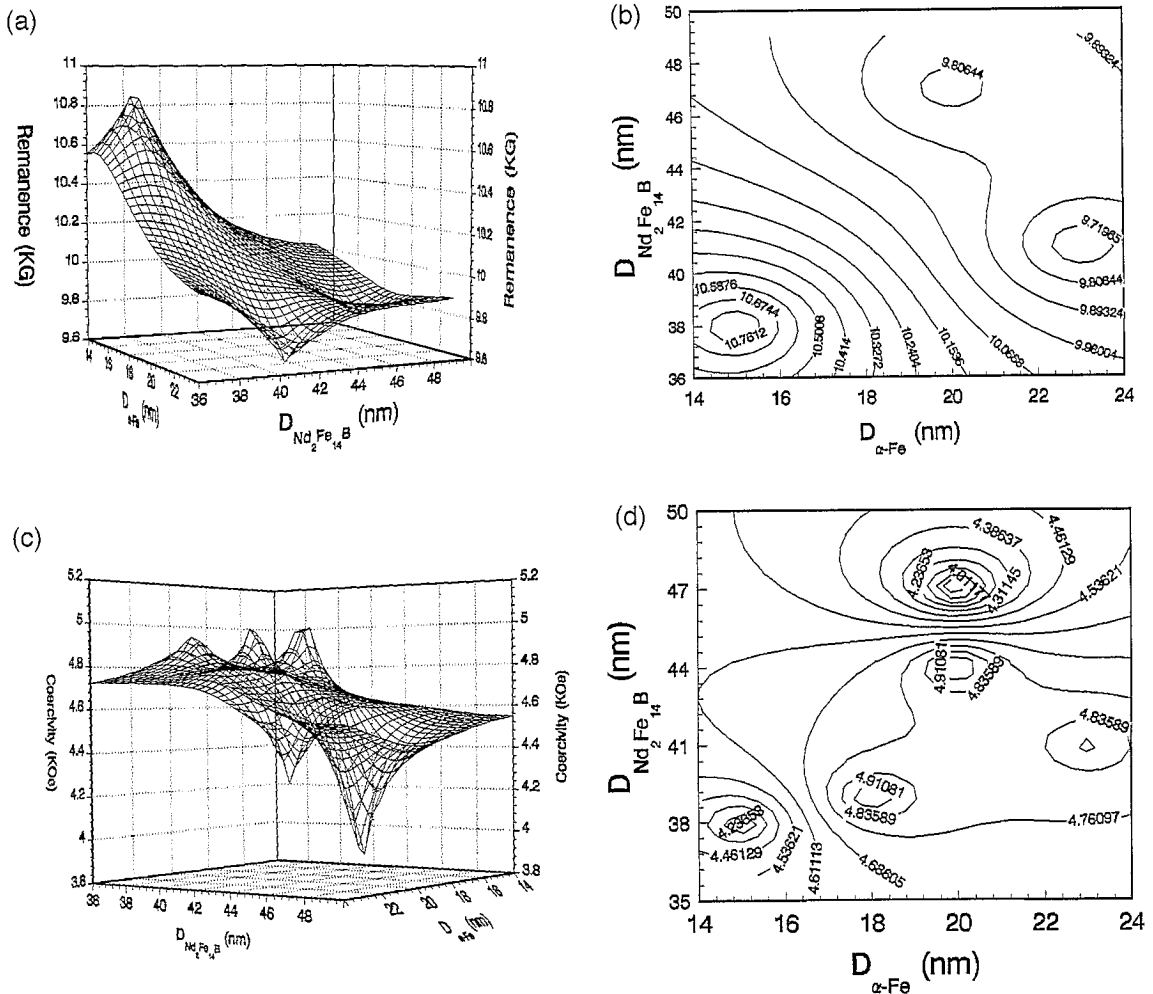


Fig. 5. Correlation between magnetic properties and grain sizes. (a) The 3D surface graph of remanence and grain sizes, (b) projected graph for (a), (c) the 3D surface graph of coercivity and grain sizes and (d) projected graph for (c).

and coercivity, H_{cj} . We also obtained a fairly linear relationship between J_r and H_{cj} , which can be expressed by

$$J_r = 1.7688 - 0.16243 \mu_0 H_{cj}.$$

Using the calculation method presented by Manaf et al. [13], we have obtained the following optimum properties:

$$J_r = 1.59 \text{ T},$$

$$H_c > 870 \text{ kA m}^{-1},$$

$$(BH)_{\max} > 400 \text{ kJ m}^{-3}.$$

These results imply that nanostructured two-phase Nd-Fe-B permanent magnets are potential candidates for application.

4. Conclusions

Remanent magnetization in excess of 1 T can be achieved in amorphous melt spun ribbons with composition $Nd_{9.32}Fe_{85.32}B_{5.36}$. After crystallization under optimized annealing conditions, an ultra-fine microstructure with mean grain sizes about 20-40 nm

can be achieved. The two-phase microstructure consists of α -Fe and Nd₂Fe₁₄B grains in which no additional metastable phase was observed. Experimental results indicate that the magnetic properties are sensitive to the microstructure for nanometer-sized specimens. With decreasing grain sizes, the residual polarization increases monotonously, while the intrinsic coercivity exhibits a “plateau region”. The presence of a “plateau region” suggests that a special grain size range (typically 15–47 nm) is required to obtain the excellent magnetic properties.

References

- [1] J.J. Croat, J.F. Herbst, R.W. Lee and F.E. Pinkerton, *J. Appl. Phys.* 55 (1984) 2078.
- [2] M. Sagawa, S. Fujimura, N. Togawa, H. Yamamoto and Y. Matsuura, *J. Appl. Phys.* 55 (1984) 2083.
- [3] N.C. Koon and B.N. Das, *J. Appl. Phys.* 55 (1984) 2063.
- [4] E.C. Stoner and E.P. Wohlfarth, *Phil. Trans. Roy. Soc.* 240 (1948) 599.
- [5] R.W. McCallum, A.M. Kadin, G.B. Clemente and J.E. Keen, *J. Appl. Phys.* 61 (1987) 3577.
- [6] R. Coehorn, D.B. Moij and C.D.E. Waard, *J. Magn. Magn. Mater.* 80 (1989) 101.
- [7] J. Ding, P.G. McCormick and R. Street, *J. Magn. Magn. Mater.* 124 (1993) 1.
- [8] R. Skomski and J.M.D. Coey, *Phys. Rev. B* 48 (1993) 15812.
- [9] T. Schrefl, J. Fidler and H. Kronmüller, *Phys. Rev. B* 49 (1994) 6100.
- [10] H. Kronmüller and T. Schrefl, *J. Magn. Magn. Mater.* 129 (1994) 66.
- [11] G.B. Clemente, J.E. Keem and J.P. Bradley, *J. Appl. Phys.* 64 (1988) 5299.
- [12] L. Withanawasam, A.S. Murphy, G.C. Hadjipanayis and R.F. Krause, *J. Appl. Phys.* 76 (1994) 7065.
- [13] A. Manaf, P.Z. Zhang, I. Ahmad, H.A. Davies and R.A. Buckley, *IEEE Trans. Mag.* 29 (1993) 2866.